

Study for pathogenesis of congenital  
cholesteatoma with comparison of  
proteins expressed in congenital  
cholesteatoma, acquired cholesteatoma  
and skin of the external auditory canal  
through proteomics

Seung Ho Shin

Department of Medicine

The Graduate School, Yonsei University

Study for pathogenesis of congenital  
cholesteatoma with comparison of  
proteins expressed in congenital  
cholesteatoma, acquired cholesteatoma  
and skin of the external auditory canal  
through proteomics

Directed by Professor Jae Young Choi

The Doctoral Dissertation  
submitted to the Department of Medicine,  
the Graduate School of Yonsei University  
in partial fulfillment of the requirements for the degree  
of Doctor of Philosophy

Seung Ho Shin

June 2014

This certifies  
that the Doctoral Dissertation of  
Seung Ho Shin is approved.



-----  
Thesis Supervisor : Jae Young Choi



-----  
Thesis Committee Member#1 : Hee-Nam Kim



-----  
Thesis Committee Member#2 : Kee Yang Chung



-----  
Thesis Committee Member#3: Jinwoong Bok



-----  
Thesis Committee Member#4: Sung Huhn Kim

The Graduate School  
Yonsei University

June 2014

## ACKNOWLEDGEMENTS

In the initial period of my fellowship, I wrote a book, Temporal Bone Dissection Manual as a coauthor with Professor Won Sang Lee, Ho-Ki Lee and Jae Young Choi. Through this book, I learned about much knowledge from them.

Professor Jae Young Choi advised me to go for a Ph.D. I admitted graduate school for a Ph.D. in 2007. In my doctoral course, he has instructed me in detail on the basic research. He has demonstrated precise and delicate laboratory techniques and showed outstanding ability to create new ideas. Also, he has often said to me that a researcher must be honest to his colleagues and even to himself.

After the summer of 2013, he gave me an idea for this paper, which was for congenital cholesteatoma analysis with proteomics. He always displayed endless energy and enthusiasm for scientific experiments even after many demanding surgeries. His passion motivated me to follow suit and seven months of our work at last bore fruit. I would like to thank him sincerely for giving me a chance to write this paper. I am especially grateful to Professor Hee-Nam Kim at the HANA ENT Hospital, Seoul, Korea, who taught me a great deal on ear surgery and has encouraged and supported me to

complete this paper. I would also like to acknowledge Professor Kee Yang Chung, Professor Jinwoong Bok and Yonsei University College of Medicine, who unhesitatingly gave me advices indispensable to this work. I am very grateful especially to Professor Sung Huhn Kim, who taught me to write this paper one by one. I also want to express my gratitude to my parents and in-laws for their special support to me and my family. I specially express my deepest gratitude to Mi Kyoung Lim, my sister in-law for her full material and spiritual support.

Finally, I would like to thank my lovely wife, Se A and my young daughters, Ji Ye and Chae Eun, for enduring the time I spent away from them while completing this paper.

## <TABLE OF CONTENTS>

ABSTRACT .....	1
I. INTRODUCTION .....	3
II. MATERIALS AND METHODS .....	5
1. Tissue Harvest .....	5
2. Preparation of samples for 2-DE .....	7
3. 2-D electrophoresis .....	7
4. Identification of protein by matrix-assisted laser desorption/ionization - time of flight mass spectrometer .....	8
5. Immunohistochemical staining .....	9
III. RESULTS .....	9
1. 2D electrophoresis of protein expression in samples of congenital cholesteatoma, acquired cholesteatoma and the skin of the external auditory canal .....	9
2. Identification of proteins in congenital cholesteatoma, acquired cholesteatoma and the skin .....	12
3. Immunohistochemical staining .....	17
IV. DISCUSSION .....	19
V. CONCLUSION .....	24
REFERENCES .....	24
ABSTRACT (IN KOREAN) .....	30

## LIST OF FIGURES

Figure 1. Otoendoscopic photo of congenital cholesteatoma behind the tympanic membrane .....	4
Figure 2. Surgical photo of congenital cholesteatoma (white arrow) during a retroauricular approach .....	5
Figure 3. Gross photo of congenital cholesteatoma .....	6
Figure 4. 2D electrophoresis with congenital cholesteatoma in 4 patients .....	10
Figure 5. 2D electrophoresis with acquired and congenital cholesteatomas .....	11
Figure 6. 2D electrophoresis with the skin of the external auditory canal and congenital cholesteatomas .....	11
Figure 7. Distribution of proteins from the congenital and acquired cholesteatomas and the skin .....	12
Figure 8. Types of proteins expressed in congenital and acquired cholesteatomas, and external auditory canal skin ·	13
Figure 9. 2-DE image of ten major spots expressed only in congenital cholesteatoma .....	14
Figure 10. 2-DE image of 8 major spots expressed only in congenital cholesteatoma .....	16
Figure 11. Immunocytochemical staining of congenital cholesteatoma using monoclonal anti-Forkhead transcriptional factor homolog (FKH 5-3) antibody .....	18

## LIST OF TABLES

Table 1. 2D electrophoresis and mass spectrum protocol .....	6
Table 2. Protein names of 10 major spots expressed only in congenital cholesteatoma .....	15
Table 3. Protein names of 8 major spots major spots which were expressed in the congenital cholesteatoma gel more than in the acquired cholesteatoma gel and not expressed in the skin gel .....	17



## ABSTRACT

Study for pathogenesis of congenital cholesteatoma with comparison of proteins expressed in congenital cholesteatoma, acquired cholesteatoma and skin of the external auditory canal through proteomics

Seung Ho Shin

*Department of Medicine  
The Graduate School, Yonsei University*

(Directed by Professor Jae Young Choi)

Congenital cholesteatomas are epithelial lesions which represent invasive growth and osteolysis. The incidence consists of 1-5 % in middle ear cholesteatoma, but the detection rate is increasing. Especially congenital cholesteatoma can make hearing function worse, when it is not properly managed. While the biochemical study of acquired cholesteatomas is progressed some degree, the pathogenesis of congenital cholesteatomas is nearly unknown. Therefore the biochemical study regarding it is necessary now. Considering limitations of genetic study, crossover analysis of proteins expressed in congenital cholesteatomas via proteomics and ELISA can give us some clue for the understanding of its pathogenesis and make progress in treatment for it. Four congenital cholesteatoma matrices, and four samples of normal external auditory canal skin and two acquired cholesteatoma were obtained intraoperatively. We performed 2D electrophoresis in order to separate the proteins by molecular weight and detected. We then analyzed the upregulated spots from the congenital cholesteatoma matrices comparing the acquired cholesteatoma specimens through MALDI-TOF MS and immunohistochemical staining.

In the 2D electrophoresis, four samples of congenital cholesteatoma showed very similar pattern of proteins expression. Comparing protein expression of acquired cholesteatoma and congenital cholesteatoma, some proteins were simultaneously expressed and the others not. Similar and different components of protein expression between the skin and congenital cholesteatoma sample were identified. The total number of spots in the 2-DE image from congenital cholesteatoma, acquired cholesteatoma and the skin was 556, 460 and 624. In the congenital and acquired

cholesteatoma 326 proteins were simultaneously expressed. Of them, 56 proteins were not expressed in the skin. In the skin and congenital cholesteatoma 373 proteins were simultaneously expressed. Therefore 127 proteins were expressed only on congenital cholesteatoma. Major spots expressed in congenital cholesteatoma gels more than in acquired cholesteatoma gels were selected and analyzed, which included titin, PRO2619, forkhead transcription activator homolog, ryanodine receptor 2, plectin 1, keratin 10 and leucine zipper protein 5. Spots which were densitometrically expressed in congenital cholesteatoma gels more than spots of acquired cholesteatoma and were not expressed in the skin gels, were analyzed. They were nine spots, which were Ig heavy chain variable region (gi|951281), chain A structure of human muscle pyruvate kinase (Pkm2, gi|67464392), ribosomal protein L35a isoform CRA\_c (gi|119612656), DNA repair and recombination protein RAD54B isoform 3 (gi|327532753), protein S100-A7 (gi|115298657), caspase-5/f (gi|81170715), chain B crystal structure of human caspase-2 in complex with Acetyl-Leu-Asp-Glu-Ser-Asp-Cho (gi|34810359) and cyclic nucleotide gated channel beta 3 (gi|223462173). In immunostaining assay, forkhead transcription activator homolog (FKH 5-3), keratin-10 and titin in congenital cholesteatoma specimen was identified in contrast to the negative control.

In this study, we found the proteins expressed in congenital cholesteatoma more than in acquired cholesteatoma. Among them, proteins which were not expressed in the skin were found. Some of them maybe play an important role in the pathogenesis of congenital cholesteatoma. But the function study for them should be continued.

---

Key words: congenital cholesteatoma, proteomic analysis, acquired cholesteatoma

# Study for pathogenesis of congenital cholesteatoma with comparison of proteins expressed in congenital cholesteatoma, acquired cholesteatoma and skin of the external auditory canal through proteomics

Seung Ho Shin

*Department of Medicine  
The Graduate School, Yonsei University*

(Directed by Professor Jae Young Choi)

## I. INTRODUCTION

Congenital cholesteatomas are epithelial lesions which are characterized with invasive growth and osteolysis.<sup>1</sup> They generally present as a whitish mass behind the tympanic membrane (Figure 1) and their incidence accounts for 1~5 % of middle ear cholesteatomas. Due to development of endoscope technique their detection rate has been recently increasing. They mostly develop from the anterosuperior quadrant of mesotympanum and the posterosuperior. The incidence of bilateral congenital cholesteatomas accounts for 4 %.<sup>2</sup> If they progress without proper treatment, they may give rise to hearing impairment. For the treatment, excision under general anesthesia is required. Figure 2 is a photo of congenital cholesteatoma in the middle ear during retroauricular approach. In case they spread out beyond their capsule in the temporal bone, wide mastoidectomy and their removal are required. Resulting complications may occur. Because affected patients are mostly children, the degree of complications can be more serious. Although many animal models for acquired cholesteatoma have been suggested, there has been no animal model for congenital cholesteatoma. The biochemical study for acquired cholesteatoma has been fairly progressed. Only a small number of reports of biochemical study for congenital cholesteatoma has been performed until now.<sup>1,3-6</sup>

It is widely known that in a cell, proteins represent the actual functional molecules and mRNA level is not correlated.<sup>7</sup> To overcome shortcomings of mRNA study, proteomics was introduced, which is the large-scale research of proteins, especially their structures and functions.<sup>8,9</sup> To the best of our knowledge, there is no report about proteomics study

for congenital cholesteatoma. Using it, we would like to analyze congenital cholesteatoma and find key molecules affecting the pathophysiology.

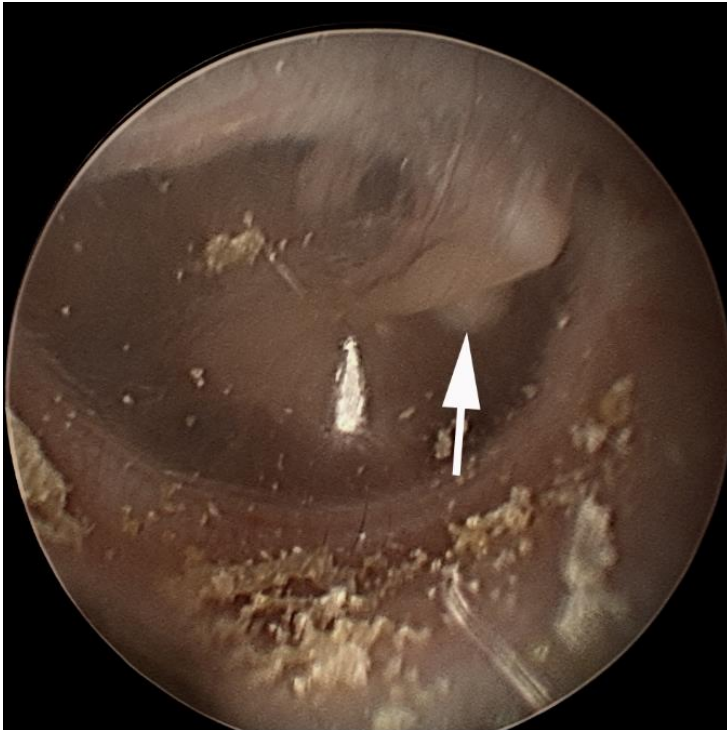


**Figure 1.** Otoendoscopic photo of congenital cholesteatoma (white arrow) behind the tympanic membrane. Congenital cholesteatoma is visible through the tympanic membrane via otoendoscopy and located anterior to the malleus handle. It is a whitish and ovoid mass like a pearl.



**Figure 2.** Surgical photo of congenital cholesteatoma (white arrow) during a retroauricular approach. The congenital cholesteatoma is visible under the chorda tympani nerve during surgery.

## II. MATERIALS AND METHODS

### 1. Tissue harvest

Patients were enrolled for the study after they provided written informed consent. We obtained approval from the local ethics committee for the use of patient specimens. Samples of congenital cholesteatoma, acquired cholesteatoma and the external auditory canal skin were harvested from patients (n =6) using a retroauricular approach. They are 4 children (3 males) with congenital cholesteatoma and 2 adults (2 females) with acquired cholesteatoma. Samples of congenital cholesteatoma were harvested without damages of its surface (Figure 3). The skin was harvested from 4 children. The samples were vigorously washed in order to take out the components of blood. Table 1 shows the steps of proteomics which will be described as below.

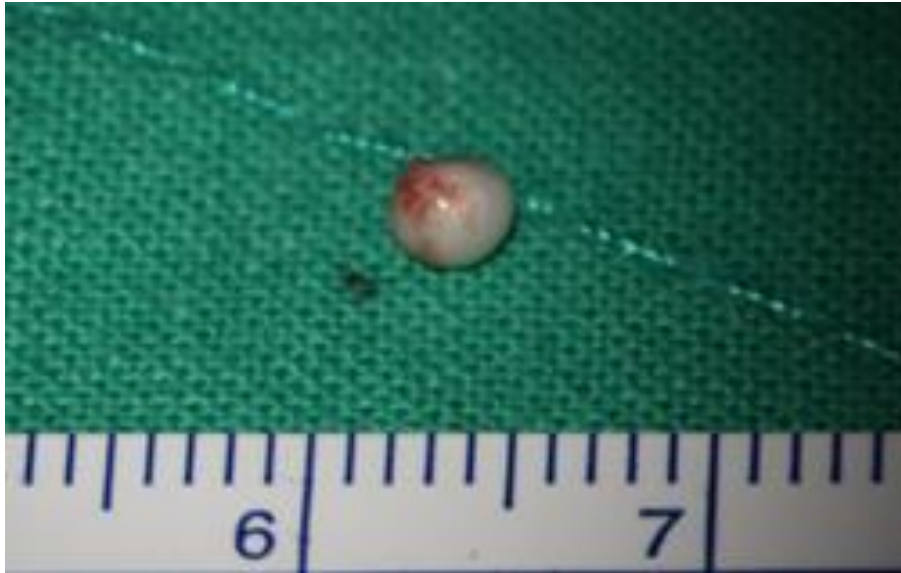


**Figure 3.** Gross photo of congenital cholesteatoma. The mass, congenital cholesteatoma is about 3 mm and has no damage by manual manipulation during surgery. For the accurate results, the specimen should be harvested without damages by surgical manipulations.

**Table 1.** 2D electrophoresis and mass spectrum protocol

<b>Procedure</b>
1. Preparation of Sample for 2-DE
2. Isoelectric Focusing (IEF)
3. Preparation of Second Dimension (2D) Gels
4. Equilibration of the Sample and Running of the Gel
5. Gel staining with Coomassie Brilliant Blue G-250
6. 2D Gel Image Analysis
7. In-gel Tryptic Digestion
8. Desalting of Peptides and MALDI Plating
9. MALDI-TOF and Peptide Mass Fingerprinting

## 2. Preparation of samples for 2-DE

Each sample was lysed with 2 × sample buffer (250 mM Tris-HCl [pH 6.5], 2 % sodium dodecyl sulfate (SDS), 1 % DTT, 0.02 % bromophenol blue, and 10 % glycerol). Protein levels were quantified by comparing the absorbance of the lysate with that of serially diluted bovine serum albumin (0, 0.2, 0.4, 0.6, 0.8, and 1 mg/ml) in the VersaMax ELISA plate reader (Molecular Devices).

## 3. 2-D electrophoresis

Isoelectric focusing (IEF) instrumentation, immobilized pH gradient gel (IPG) strips (18 cm; pH 3-10) and related reagents were purchased from BioRad. IPG strips were rehydrated and focused during an automated overnight run in ceramic strip holders using 8 h of rehydration, followed by 1 h each at 500, 1000 and 2000 V, followed by 9 h 20 min at 5000 V for a total of 50 kVh. Immediately prior to loading the focused IPG strips on the 2D gels, the strips were incubated in equilibrium buffer (6 M urea, 10% sodium dodecylsulfate [SDS], Tris, pH 8.8, glycerol and dithiothreitol [DTT]) for 15 min, followed by incubation for 15 min in the same solution, except that the DTT was replaced by iodoacetamide. 2D SDS polyacrylamide gel electrophoresis (PAGE) 12% gels (acrylamide/bis 30% acrylamide/bis, distilled water, 1.5 M Tris/HCl, pH 8.8, 10% SDS, 10% ammonium persulfate, 0.1% tetra-methyl-ethylenediamine) were cast with glass plate sandwiches from Bio-Rad Protean II xi chambers (20X20 cm<sup>2</sup>; 1.5-mm thick). The SDS equilibrated IPGs were sealed on top of the 2D gels using 0.5% agarose containing bromophenol blue. SDS gels were run until the tracking dye was within 1 cm of the gel bottom. Colloidal CBB staining was used to visualize proteins and gel images were scanned. Silver staining was conducted as described by Hochstrasser et al.<sup>10</sup> Stained 2D gels were analyzed using Melanie III 2D PAGE analysis software (Genebio, Geneva, Switzerland). Congenital cholesteatoma matrix gels were compared with three normal external auditory canal skin gels and acquired cholesteatoma gels. Spots upregulated in congenital cholesteatoma gels, or only detected in congenital cholesteatoma densitometrically were selected and analyzed.

#### 4. Identification of protein by matrix-assisted laser desorption/ionization - time of flight mass spectrometer (MALDI-TOF MS)

For 2-D gel mapping, major proteins were identified by mass finger printing or by matching with various internal 2-DE maps. Protein spots excised from 2-DE gels were destained, reduced, alkylated and digested with trypsin (Promega, Madison, WI) as previously described.<sup>11</sup> For MALDI-TOF MS analysis, the peptides were concentrated by a POROS R2, Oligo R3 column (Applied Biosystems, Foster city, CA, USA). After washing the column with 70% acetonitrile, 100% acetonitrile and then 50 mM ammonium bicarbonate, samples were applied to the R2, R3 column and eluted with cyano-4-hydroxycinamic acid (CHCA) (Sigma, St. Louis, MO) dissolved in 70% acetonitrile and 2% formic acid onto the MALDI plate (Opti-TOF™ 384-well Insert, Applied Biosystems).<sup>12</sup> MALDI-TOF MS was performed on 4800 MALDI-TOF/TOF™ Analyzer (Applied Biosystems) equipped with a 355-nm Nd:YAG laser. The pressure in the TOF analyzer is approximately  $7.6 \times 10^{-7}$  Torr. The mass spectra were obtained in the reflectron mode with an accelerating voltage of 20 kV and sum from either 500 laser pulses and calibrated using the 4700 calibration mixture (Applied Biosystems). Proteins were identified from the peptide mass maps using MASCOT ([http://www.matrixscience.com/search\\_form\\_select.html](http://www.matrixscience.com/search_form_select.html)), which searched the protein databases of the NCBI non-redundant human database containing 115818 entries (downloaded on 05/09/2009).

##### A. Analysis of upregulated proteins in congenital cholesteatoma comparing acquired cholesteatoma

Top ten spots of which were expressed in congenital cholesteatoma gels more than paired spots in acquired cholesteatoma gels were selected and analyzed,

##### B. Analysis of major spots expressed only in congenital cholesteatoma

To find the proteins expressed only in congenital cholesteatoma, paired spots in skin gels were excluded among the upregulated spots in congenital cholesteatoma gels. Top nine spots were selected and analyzed.



## 5. Immunohistochemical staining

To examine the expression pattern of target proteins, tissues were fixed with 4% paraformaldehyde for 24 hours and then dehydrated and embedded in paraffin. Paraffin blocks were sectioned into 5- $\mu$ m-thick slices and fixed with a chilled 1:1 mixture of methanol and acetone for 5 minutes after pretreatment with 0.3% H<sub>2</sub>O<sub>2</sub> for 20 minutes at room temperature. Slides were treated with 1:600 normal rabbit serum for 20 minutes to block nonspecific reactions and then incubated with a monoclonal mouse antibody against target proteins including Titin (HPA007042, sigma<sup>®</sup>), forkhead transcription activator homolog (clone FKH 5-3, human (fragment), AHP933, AbD Serotec<sup>®</sup>) and keratin10 (ab97764, abcam<sup>®</sup>). The slides were then incubated with biotinylated antimouse rabbit immunoglobulin G (1:200; Vector Laboratories<sup>®</sup>, Burlingame, CA, USA). Peroxidase was attached to the secondary antibody by avidin-biotin peroxidase complex formation. Specimens were incubated in diaminobenzidine tetrahydrochloride to detect primary antibody binding sites.

## III. RESULTS

### 1. 2D electrophoresis of protein expression in samples of congenital cholesteatoma, acquired cholesteatoma and the skin of the external auditory canal

In the 2D electrophoresis, four samples of congenital cholesteatoma showed very similar pattern of proteins expression (Figure 4). Comparing protein expression of acquired cholesteatoma and congenital cholesteatoma, some proteins were simultaneously expressed and the others not (Figure 5). Similar and different components of protein expression between the skin and congenital cholesteatoma sample were identified (Figure 6). To sum it up, we could make a diagram (Figure 7), which meant the distribution of expressed proteins among the samples. The proteins which expressed only in congenital cholesteatoma maybe play an important role in the pathogenesis of congenital cholesteatoma. Also among proteins which simultaneously expressed in congenital and acquired cholesteatomas, overexpressed ones maybe effect on the pathogenesis.

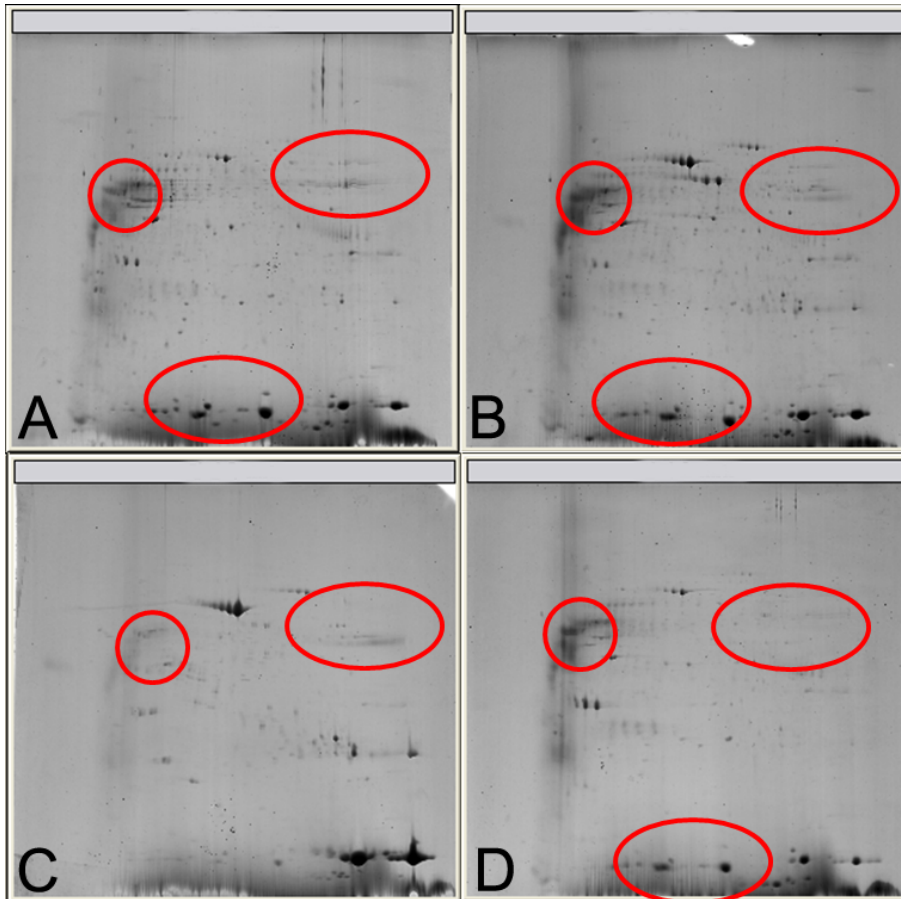


**Figure 4.** 2D electrophoresis with congenital cholesteatoma in 4 patients (A-D). In the Figure A-D, the similar pattern (red circles) is visible. This means that congenital cholesteatoma in each patients shows same pattern of proteins expression in 2D electrophoresis.

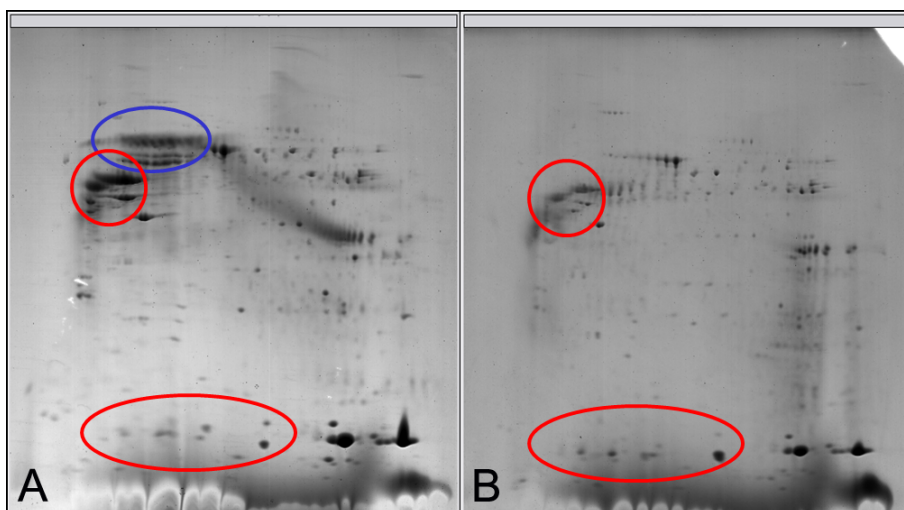


**Figure 5.** 2D electrophoresis with acquired (A) and congenital (B) cholesteatomas. Red circles shows similar pattern of proteins expression between acquired and congenital cholesteatomas and blue circle means the proteins expressed in acquired cholesteatoma.

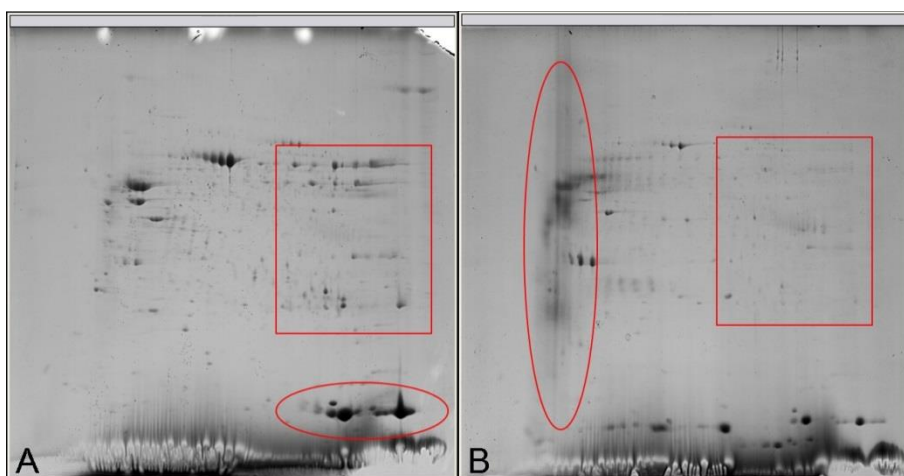


**Figure 6.** 2D electrophoresis with the skin of the external auditory canal (A) and congenital cholesteatomas (B). Two of 2D electrophoresis show similar pattern in some region and different in the other. Number of spots in congenital cholesteatoma is less than in the skin.

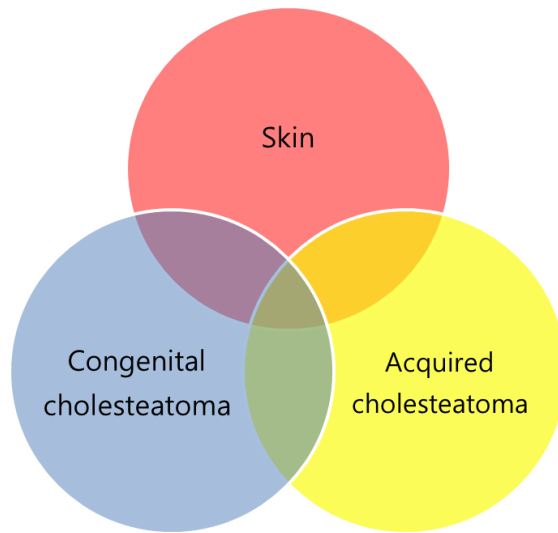


**Figure 7.** Distribution of proteins from the congenital and acquired cholesteatomas and the skin. Based on the Figure 4, 5 and 6, it is inferred that distribution of proteins is as above diagram. That is, 3 specimens have common proteins and also their own.

## 2. Identification of proteins in congenital cholesteatoma, acquired cholesteatoma and the skin

MALDI-TOF MS was performed to identify the proteins represented by each spot in the 2-DE of congenital cholesteatoma 1. The total number of spots in the 2-DE image from congenital cholesteatoma, acquired cholesteatoma and the skin was 556, 460 and 624 (Figure 8). In the congenital and acquired cholesteatoma 326 proteins were simultaneously expressed. Of them, 56 proteins were not expressed in the skin. In the skin and congenital cholesteatoma 373 proteins were simultaneously expressed. Therefore 127 proteins were expressed only on congenital cholesteatoma.

Ten major spots densitometrically expressed in the congenital cholesteatoma gel more than in the acquired cholesteatoma gels were selected and analyzed, which included titin (gi|407139), PRO2619 (gi|11493459), forkhead transcription activator homolog (gi|477361), ryanodine receptor 2 isoform CRA\_c (gi|119590477), plectin 1 intermediate filament binding protein (gi|119602578), , keratin 10 (epidermolytic hyperkeratosis; keratosis palmaris et plantaris, gi|119581085), keratin 10 (gi|186629),

keratin 10 (gi|119581085), titin (gi|407139) and leucine zipper protein 5 isoform CRA\_b (gi|119624991). These results are shown in Figure 9 and Tables 2.

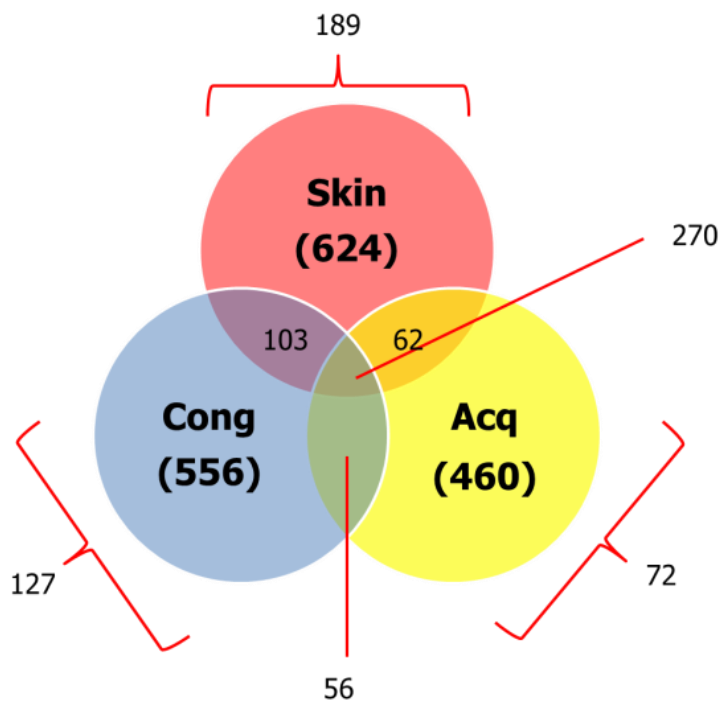


**Figure 8.** Types of proteins expressed in congenital and acquired cholesteatomas, and external auditory canal skin.

Skin: proteins expressed in external auditory canal skins, Cong: proteins expressed in congenital cholesteatomas, Acq: proteins expressed in acquired cholesteatoma

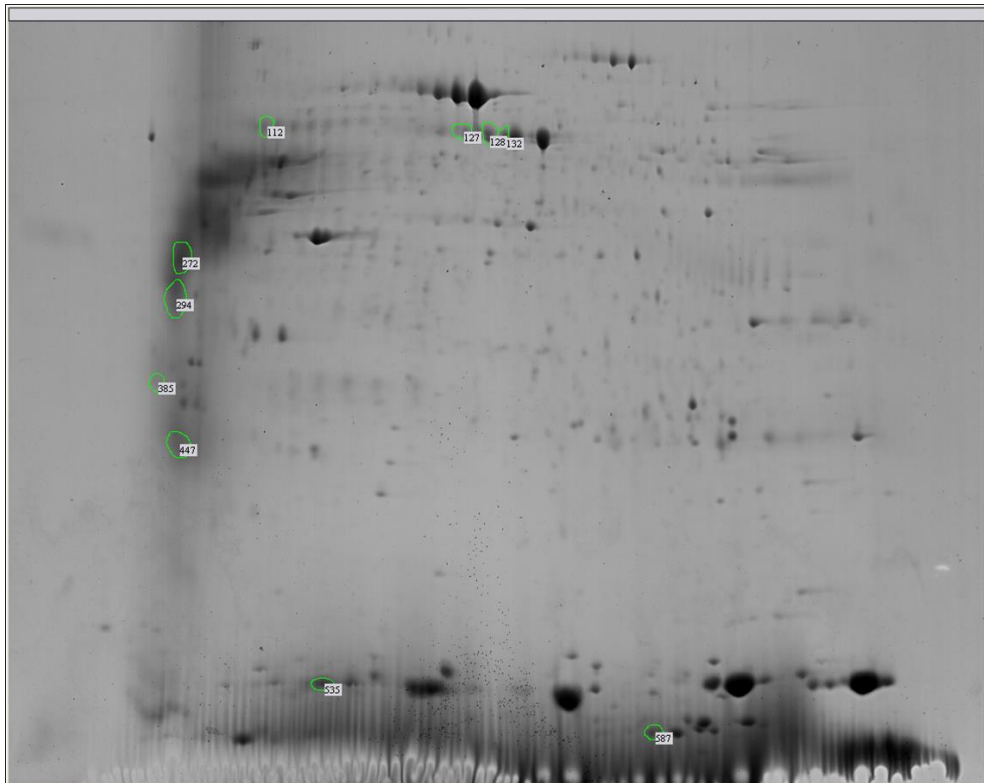


**Figure 9.** 2-DE image of ten major spots expressed in congenital cholesteatoma.

**Table 2.** Protein names of 10 major spots expressed in congenital cholesteatoma gel more than in acquired cholesteatoma gel

Group No.	Protein name (gray p>0.05)	M <sub>r</sub>	PI	% coverage	Matched peptide number
112	68 for gi 407139, titin	524823	8.06	10	28
127	66 for gi 11493459, PRO2619)	58513	5.96	21	15
128	66 for gi 477361, clone FKH 5-3	12861	10.06	66	5
132	67 for gi 119590477, ryanodine receptor 2 (cardiac) isoform CRA_c	568496	5.69	10	28
272	67 for gi 119602578, plectin 1 intermediate filament binding protein isoform CRA_c	290791	5.62	14	41
294	81 for gi 119581085, keratin 10	63536	5.13	28	16
385	66 for gi 186629, keratin 10	39832	4.72	31	10
447	77 for gi 119581085, keratin 10	63536	5.13	30	16
535	67 for gi 407139, titin	524823	8.06	11	29
587	66 for gi 119624991, leucine zipper protein 5 isoform CRA_b	9456	11.70	72	8

Mr: nominal mass, FKH: Forkhead transcriptional factor, PI: calculated pI value, % coverage: sequence coverage, Matched peptide number: number of mass values matched

Spots which were densitometrically upregulated in congenital cholesteatoma gels comparing spots of acquired cholesteatoma and simultaneously were not expressed in the skin gels, were analyzed. They were nine spots, which were Ig heavy chain variable region (gi|951281), chain A structure of human muscle pyruvate kinase (Pkm2, gi|67464392), ribosomal protein L35a isoform CRA\_c (gi|119612656), DNA repair and recombination protein RAD54B isoform 3 (gi|327532753), protein S100-A7 (gi|115298657), caspase-5/f (gi|81170715), chain B crystal structure of human caspase-2 in complex with Acetyl-Leu-Asp-Glu-Ser-Asp-Cho (gi|34810359) and cyclic nucleotide gated channel beta 3 (gi|223462173). These results are shown in Figure 10 and Tables 3.

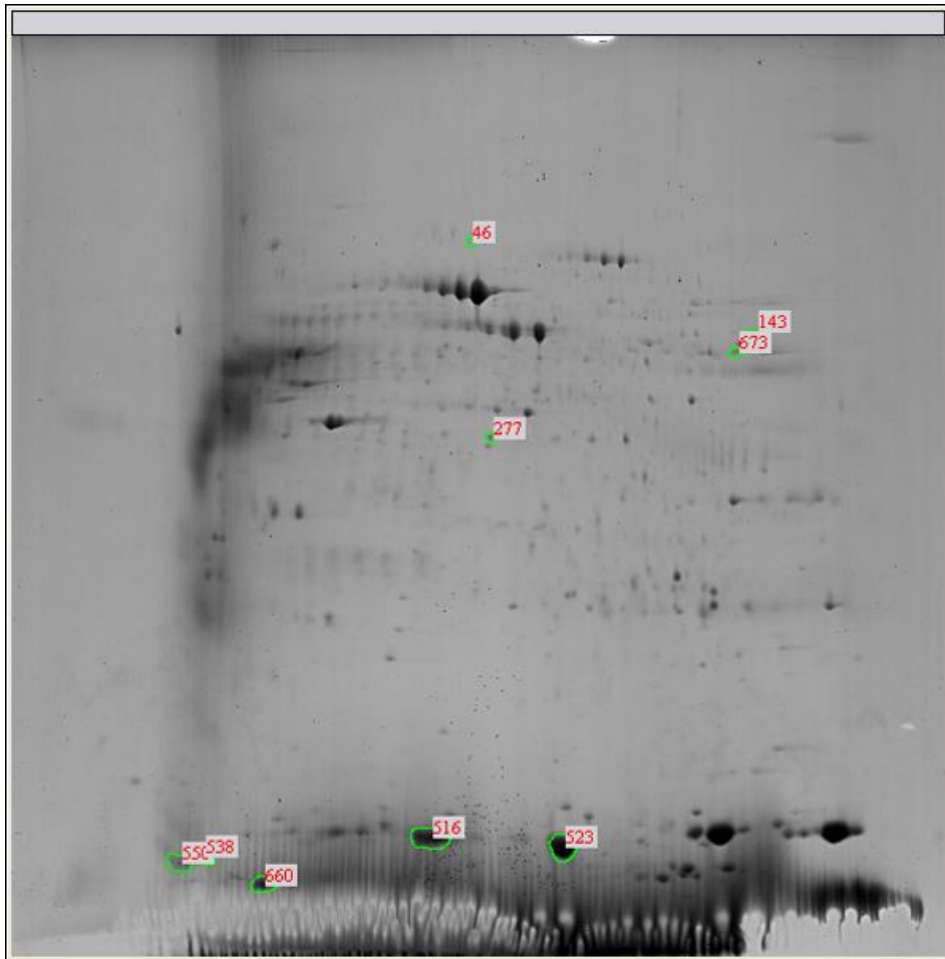


**Figure 10.** 2-DE image of 9 major spots expressed only in congenital cholesteatoma.



**Table 3.** Protein names of 9 major spots major spots which were expressed in the congenital cholesteatoma gel more than in the acquired cholesteatoma gel and not expressed in the skin gel.

Group No.	Protein name (gray p>0.05)	M <sub>r</sub>	PI	% coverage	Matched peptide number
46	35 for gi 951281, Ig heavy chain variable region	14247	9.44	55	4
143	66 for gi 67464392, Chain A Structure Of Human Muscle Pyruvate Kinase (Pkm2)	60277	8.22	25	11
277	66 for gi 119612656, ribosomal protein L35a, isoform CRA_c	16121	11.19	52	9
516	66 for gi 327532753, DNA repair and recombination protein RAD54B isoform 3	83786	8.03	31	13
523	72 for gi 115298657, protein S100-A7	11578	6.28	68	10
538	68 for gi 81170715, caspase-5/f	51785	9.28	31	9
550	34 for gi 34810359, Chain B Crystal Structure Of Human Caspase-2 In Complex With Acetyl-Leu-Asp-Glu-Ser-Asp-Cho	12235	8.98	58	5
660	68 for gi 223462173, Cyclic nucleotide gated channel beta 3	92633	8.37	20	12
673	66 for gi 55960204, UBX domain protein	18324	8.56	22	8

Mr: nominal mass, PI: calculated pI value, % coverage: sequence coverage, Matched peptide number: number of mass values matched

### 3. Immunohistochemical staining

Immunolocalization demonstrated that Forkhead transcriptional factor homolog (FHK 5-3) localized in the cell membrane and cytoplasm in all layers of keratinocytes of congenital cholesteatoma in contrast to the negative control. Figure 11. A shows the distribution of Forkhead transcriptional factor homolog protein in keratinocytes. Control studies using normal IgG instead of primary antibody all showed no staining in congenital cholesteatoma. Figure 11. B shows the negative control. Also keratin-10 and titin were also identified in congenital cholesteatoma specimen.

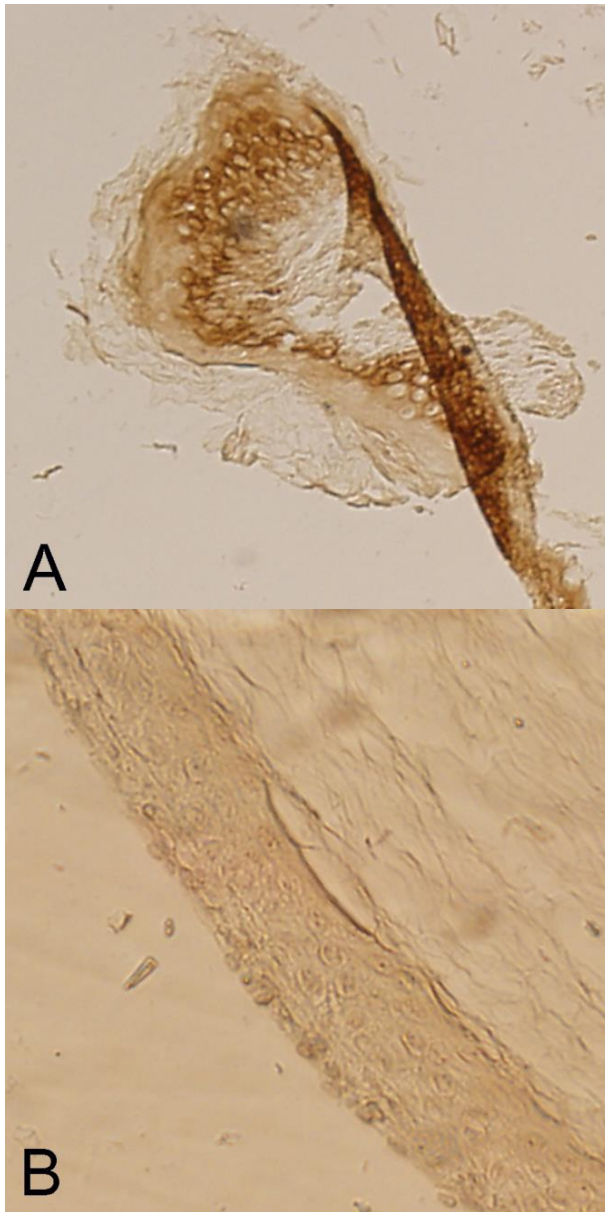


**Figure 11.** Immunocytochemical staining of congenital cholesteatoma using monoclonal anti-Forkhead transcriptional factor homolog (FKH 5-3) antibody. A. A positive brown staining is visible in the keratinocytes in the congenital cholesteatoma epithelium, B. Negative control.

## IV. DISCUSSION

### Definition and incidence of congenital cholesteatoma

In 1953, the first case of congenital cholesteatoma was reported by Howard House.<sup>13</sup> Derlacki and Clemis presented 6 cases of congenital cholesteatoma and established the clinical criteria for the diagnosis.<sup>14</sup> These includes a whitish mass medial to an intact tympanic membrane, a normal pars tensa and flaccida, and ho history of otorrhea, perforation or previous otologic procedure.<sup>15</sup>

The detection rate of congenital cholesteatomas originated from the middle ear cavity has been increased and accounts for 2% to 5%.<sup>16</sup> Therefore many otologists are becoming interested in them. Based on the position and stage of them, their symptoms and signs include conductive hearing loss, sensorineural hearing loss, facial palsy, labyrinthitis and intracranial complications.

### Proposed pathophysiology

The pathophysiology of congenital cholesteatomas of the middle ear is still controversial. Suggested mechanisms are epithelial rests from faulty embryogenesis, invagination of squamous epithelium, implantation, or metaplasia of normal epithelium.<sup>15</sup>

Among them, epithelial rest theory is the most commonly accepted. Teed reported a small splinter of epidermal cells which showed cornification and desquamation and was in the dorsolateral pole of the tympanum, just medial to the neck of the malleus in 5.5-month fetus. He trusted that normally epidermal cells become transformed into epithelial cells but sometimes they persist in their ectodermal quality and produce skin, which finally result in cholesteatoma.<sup>17</sup> In 1997, Kayhan et al investigated 226 fetal, neonatal and children's temporal bones.<sup>18</sup> They noticed 25 epidermoid formations without keratinization in fetal, infantal and children's temporal bones.

Invagination theory, that is, migration of normal squamous epithelium from the external auditory canal through the annulus and into the middle ear as the pathophysiology of congenital cholesteatoma was suggested by Ruedi and Aimi.<sup>19,20</sup> Their theory is that due to small inflammatory injury of the epithelium, invagination of the epithelium can occur and form a congenital cholesteatoma. It doesn't have been supported by histopathologic evidence, but would explain lesions not located in the anterior superior quadrant of the tympanic membraine.<sup>15</sup>

Implantation theory was proposed by Friedberg and Sheehy, which was that implantation of squamous epithelium by trauma and subsequent healing of the tympanic membrane

resulted in the formation of congenital cholesteatoma.<sup>21,22</sup> It may explain some cases of congenital cholesteatoma, which arises from many different sites but is incompatible with the definition of congenital cholesteatoma.

Metaplasia theory was advocated by Sade.<sup>6</sup> It means that the inflamed middle ear epithelium is converted into the squamous epithelium, but cannot explain the high frequency of cholesteatoma lesions in the anterior superior quadrant of middle ear.

#### Animal Model for cholesteatoma

Many animal models for acquired cholesteatoma were reported in the literature. Ruedi reported that cholesteatoma was induced due to application of mixture with talc and fibrin into the inner surface of the tympanic membrane in the Guinea pig model.<sup>20</sup> Friedmann observed the external auditory canal skin moved into the middle ear through the perforation after injection of bacteria into the tympanic cavity in the Guinea pig model.<sup>23</sup> Abramson, Jackson and Lim demonstrated that cholesteatoma occurred after the fragment of the skin was implanted into the middle ear of guinea pigs and cat model, respectively.<sup>24,25</sup> Steinbach reported the rabbit model, in which he observed cholesteatoma growth secondary to the operative closure of the external auditory canal.<sup>26</sup> Wright suggested the chinchilla middle ear model in which cholesteatoma appeared after injection of the propylene glycol into the middle ear.<sup>27</sup> Wolfman and Chole made Mongolian gerbil model in which they showed retraction pocket formation after electrocauterization of the Eustachian tube. However, there has been no animal model for congenital cholesteatoma so far.

#### Current biochemical study's advances for congenital cholesteatoma

Though modern biochemical research for many diseases has been well developed, the exact pathogenic molecular mechanism of congenital cholesteatoma remains unclear.

In 1992, Immunohistochemical study to determine the pattern of cytokeratin expression in congenital and acquired cholesteatoma was reported By Broekaert et al. They showed same cytokeratin expression.<sup>28</sup> In addition, Olszewska et al reported the same result with Broekaert.<sup>3</sup>

In 1993, number of dendritic cells in acquired and congenital cholesteatoma was compared by Frankel et al.<sup>5</sup> They observed congenital cholesteatoma specimen significantly had smaller number of dendritic cells than acquired cholesteatoma did and stated that congenital cholesteatomas are pathologically different entity from acquired cholesteatoma.

Ras protein modulating cellular proliferation, transformation and differentiation was identified in both congenital and acquired cholesteatomas by Huang et al.<sup>29</sup> They think it might play a pivotal role in a signal transduction cascade.

Expression of P53 tumor suppressor gene regulating cell cycle control and apoptosis in acquired and congenital cholesteatoma was elevated 9 to 20 folds when compared to the expression of p53 in normal external auditory canal skin.<sup>30</sup>

Tumor necrosis factor-alpha regulating bone resorption and cell infiltration was studied, of which expression was increased in both congenital and acquired cholesteatoma as compared to normal skin.<sup>31</sup>

Kojima et al studied about telomere length in both cholesteatomas and found that telomere length of congenital cholesteatoma was shorter than one of normal skin and the length of acquired cholesteatoma almost the same as in the normal external ear canal skin.<sup>32</sup> This study support the epithelial rest theory which was described above.

The decreased p27 protein levels in both cholesteatomas were reported. The authors concluded that its role was unclear but its level could influence the proliferative state.<sup>33</sup>

Park et al studied p63 and survivin.<sup>34</sup> p63 overexpression which was related to actively proliferative cells was observed in congenital cholesteatoma. Survivin, a potential modulator of keratinocyte apoptosis is was noted focally in the basal layer or not noted at all in congenital cholesteatoma. The authors concluded that the theory that congenital cholesteatoma originates from vestigial fetal tissue or aberrant tissue.

IL-17 which induces the production of inflammatory cytokines such as IL-1, TNF-alpha and IL-1 was analyzed for congenital cholesteatoma by Haruyama et al.<sup>35</sup> They reported IL-17-driven pathology was found in both cholesteatoma.

Ki-67 in congenital cholesteatoma was studied by Sikka et al.<sup>36</sup> It is widely used proliferation marker in tumors. The authors tried to find the relationship between Ki-67 and aggressiveness of acquired and congenital cholesteatoma but there was no difference between them.

In 2013, Olszewska et al reported that p21 and p53 expression in congenital cholesteatoma.<sup>1</sup> They are related to apoptosis. The authors concluded that upregulation of p21 protein is expected to a significant role in congenital cholesteatoma development.

In summary, current trends of biochemical study for congenital cholesteatoma has focused on the apoptosis of keratinocytes.

## Present study

Among the proposed theories as described before, we focused on the epithelial cell rest theory. Michales et al investigated 68 fetal temporal bones, found the epithelial cell rest from the middle ears only before the 33<sup>rd</sup> week of gestation and speculated they would disappear or decrease in size with increasing age.<sup>37-40</sup> On the contrary, Kayhan et al examined 226 fetal temporal bones and found the size of epithelial cell rest increased with increasing age. They concluded an epithelial cell rest may cease in late fetal life but may remain in some. Therefore it is thought that there is an unknown mechanism which may influence on continuance of an epithelial cell rest after 33<sup>rd</sup> weeks of gestation.

To find unknown mechanism, proteomics study was used in this study. It is a useful tool for separating proteins and quantitatively comparing changes in protein components between each tissues.<sup>41</sup> For comparison of the materials, congenital cholesteatoma, the skin of the external auditory canal, and acquired cholesteatoma were selected. With two dimensional gel electrophoresis, proteins were separated. The pattern of protein distribution among 4 congenital cholesteatomas after gel electrophoresis was relatively similar contrary to expectations (Figure 4). In the present study, 127 proteins expressed only in congenital cholesteatoma were found.

Top ten upregulated proteins which were found in congenital cholesteatoma and expressed more than in acquired cholesteatoma, were selected for MALDI-TOF and MASCOT analysis. They were revealed as titin (gi|407139), PRO2619 (gi|11493459), forkhead transcription activator homolog (gi|477361), ryanodine receptor 2 (cardiac), isoform CRA\_c (gi|119590477), plectin 1, intermediate filament binding protein (gi|119602578), , keratin 10 (epidermolytic hyperkeratosis; keratosis palmaris et plantaris, gi|119581085), keratin 10 (gi|186629), keratin 10 (gi|119581085), titin (gi|407139) and leucine zipper protein 5 isoform CRA\_b (gi|119624991). Among them, keratin components were excluded for candidate proteins. It is know that titin seems play a role in chromosome condensation and chromosome segregation during mitosis.<sup>42</sup> ryanodine receptor 2 is calcium channel that mediates the release of Ca<sup>2+</sup> from the sarcoplasmic reticulum into the cytoplasm and plays a key role in triggering cardiac muscle contraction.<sup>43,44</sup> There has been no report it is related to keratinocytes. Leucine zipper protein has a common three-dimensional structural motif in proteins. These motifs are usually found as part of a DNA-binding domain in various transcription

factors, and are therefore involved in regulating gene expression.<sup>45</sup> Plectin 1 is interlinks intermediate filaments with microtubules and microfilaments and anchors intermediate filaments to desmosomes or hemidesmosomes.<sup>46,47</sup>

Forkhead (FKH) gene is a new family of transcriptional factors that regulate development and are related to immune response.<sup>48</sup> Some of them regulate T cells and B cells and promote and/or maintain chronic inflammation by preserving inflammatory leukocyte survival and/or otherwise promoting the expression of inflammatory target genes, at least in some cell types such as neutrophils.<sup>49</sup> There is a report that forkhead transcription factors can influence on cholesteatoma growth and proliferation via Akt/PKB pathway activation and subsequent apoptosis inhibition.<sup>50</sup> Among its family, it is known that FKH 5-3 was found in blood cells including CML cell line K562 and in the Jurkat T-cell leukemia line but not normal human marrow.<sup>51,52</sup> It is related to early hematopoietic development.<sup>48</sup> There is no report that FKH 5-3 is associated with other tissues.

Top nine upregulated proteins which were found in congenital cholesteatoma and expressed more than in acquired cholesteatoma but were not expressed in the skin specimen, were selected for MALDI-TOF and MASCOT analysis. They were revealed as Ig heavy chain variable region (gi|951281), chain A structure of human muscle pyruvate kinase (Pkm2, gi|67464392), ribosomal protein L35a isoform CRA\_c (gi|119612656), DNA repair and recombination protein RAD54B isoform 3 (gi|327532753), protein S100-A7 (gi|115298657), caspase-5/f (gi|81170715), chain B crystal structure of human caspase-2 in complex with Acetyl-Leu-Asp-Glu-Ser-Asp-Cho (gi|34810359) and cyclic nucleotide gated channel beta 3 (gi|223462173). It is thought that Ig heavy chain variable region, ribosomal protein L35a isoform CRA\_c, crystal structure of human caspase-2 in complex with Acetyl-Leu-Asp-Glu-Ser-Asp-Cho, cyclic nucleotide gated channel beta 3 and UBX domain protein 11 may not related to the pathophysiology for congenital cholesteatoma based on the proteomics database. Pkm2 is a glycolytic enzyme that catalyzes the transfer of a phosphoryl group from phosphoenolpyruvate (PEP) to ADP, generating ATP. It plays a general role in caspase independent cell death of tumor cells. The transition between the 2 forms contributes to the control of glycolysis and is important for tumor cell proliferation and survival.<sup>53-55</sup> DNA repair and

recombination protein RAD54B isoform 3 involves in DNA repair and mitotic recombination.<sup>56,57</sup> Protein S100-A7 is a member of the S100 family of proteins containing 2 EF-hand calcium-binding motifs. S100 proteins involved the regulation of a number of cellular processes such as cell cycle progression and differentiation.<sup>58</sup> This protein is markedly over-expressed in the skin lesions of psoriatic patients. It is found in fetal ear and the skin and has antimicrobial properties.<sup>59</sup> Therefore it may be related to the epithelial rest theory. Caspase-5/f is a mediator of programmed cell death, that is, apoptosis.<sup>60</sup> As mentioned above, the pathophysiology of cholesteatoma recently proposed is apoptosis. Therefore caspase-5/f may have an important role for the pathophysiology.

In summary, several candidate proteins were identified but further study is required in order to find the exact proteins which act as a key protein in the pathophysiology of congenital cholesteatoma.

## V. CONCLUSION

In this study, we found the proteins expressed only in congenital cholesteatoma in contrast with acquired cholesteatoma or the skin. They maybe play an important role in the pathogenesis of congenital cholesteatoma. But the function study for them should be continued.

## REFERENCES

1. Olszewska E, Rutkowska J, Minovi A, Sieskiewicz A, Rogowski M, Dazert S. The Role of p21 and p53 Proteins in Congenital Cholesteatoma. *Otol Neurotol* 2013;34:266-74.
2. Friedberg J. Congenital cholesteatoma. In: Lalwani AK, Grundfast K, editors. *Pediatric otology and neurotology*. Philadelphia: Lippincott-Raven; 1998.
3. Olszewska E, Lautermann J, Koc C, Schwaab M, Dazert S, Hildmann H, et al. Cytokeratin expression pattern in congenital and acquired pediatric cholesteatoma. *Eur Arch Otorhinolaryngol* 2005;262:731-6.
4. Bernal-Sprekelsen M, Sudhoff H, Hildmann H. Evidence against neonatal aspiration of keratinizing epithelium as a cause of congenital cholesteatoma.



- Laryngoscope 2003;113:449-51.
5. Frankel S, Berson S, Godwin T, Han JC, Parisier SC. Differences in dendritic cells in congenital and acquired cholesteatomas. *Laryngoscope* 1993;103:1214-7.
  6. Sade J, Babiacki A, Pinkus G. The metaplastic and congenital origin of cholesteatoma. *Acta Otolaryngol* 1983;96:119-29.
  7. Rogers S, Girolami M, Kolch W, Waters KM, Liu T, Thrall B, et al. Investigating the correspondence between transcriptomic and proteomic expression profiles using coupled cluster models. *Bioinformatics* 2008;24:2894-900.
  8. Anderson NL, Anderson NG. Proteome and proteomics: new technologies, new concepts, and new words. *Electrophoresis* 1998;19:1853-61.
  9. Blackstock WP, Weir MP. Proteomics: quantitative and physical mapping of cellular proteins. *Trends Biotechnol* 1999;17:121-7.
  10. Hochstrasser DF, Patchornik A, Merrill CR. Development of polyacrylamide gels that improve the separation of proteins and their detection by silver staining. *Anal Biochem* 1988;173:412-23.
  11. Shevchenko A, Wilm M, Vorm O, Mann M. Mass spectrometric sequencing of proteins silver-stained polyacrylamide gels. *Anal Chem* 1996;68:850-8.
  12. Choi BK, Cho YM, Bae SH, Zoubaulis CC, Paik YK. Single-step perfusion chromatography with a throughput potential for enhanced peptide detection by matrix-assisted laser desorption/ionization-mass spectrometry. *Proteomics* 2003;3:1955-61.
  13. House HP. An apparent primary cholesteatoma; case report. *Laryngoscope* 1953;63:712-3.
  14. Derlacki EL, Clemis JD. Congenital cholesteatoma of the middle ear and mastoid. *Ann Otol Rhinol Laryngol* 1965;74:706-27.
  15. Bennett M, Warren F, Jackson GC, Kaylie D. Congenital cholesteatoma: theories, facts, and 53 patients. *Otolaryngol Clin North Am* 2006;39:1081-94.
  16. Paparella MM, Rybak L. Congenital cholesteatoma. *Otolaryngol Clin North Am* 1978;11:113-20.
  17. Teed RW. Cholesteatoma verum tympani - Its relationship to the first epibranchial placode. *Arch Otolaryngol* 1936;24:455-74.
  18. Kayhan FT, Mutlu C, Schachern PA, Le CT, Paparella MM. Significance of epidermoid formations in the middle ear in fetuses and children. *Arch Otolaryngol Head Neck Surg* 1997;123:1293-7.
  19. Aimi K. Role of the tympanic ring in the pathogenesis of congenital cholesteatoma. *Laryngoscope* 1983;93:1140-6.
  20. Ruedi L. Cholesteatoma formation in the middle ear in animal experiments. *Acta Otolaryngol* 1959;50:233-40; discussion 40-2.
  21. Friedberg J. Congenital cholesteatoma. *Laryngoscope* 1994;104:1-24.
  22. House JW, Sheehy JL. Cholesteatoma with intact tympanic membrane: a report of 41 cases. *Laryngoscope* 1980;90:70-6.
  23. Friedmann I. The comparative pathology of otitis media, experimental and human. II. The histopathology of experimental otitis of the guinea-pig with particular reference to experimental cholesteatoma. *J Laryngol Otol* 1955;69:588-601.
  24. Abramson M, Asarch RG, Litton WB. Experimental aural cholesteatoma

- causing bone resorption. *Ann Otol Rhinol Laryngol* 1975;84:425-32.
25. Jackson DG, Lim DJ. Fine morphology of the advancing front of cholesteatoma--experimental and human. *Acta Otolaryngol* 1978;86:71-88.
  26. Steinbach E, Gruninger G. Experimental production of cholesteatoma in rabbits by using non-irritants (skin tolerants). *J Laryngol Otol* 1980;94:269-79.
  27. Wright CG, Meyerhoff WL, Burns DK. Middle ear cholesteatoma: an animal model. *Am J Otolaryngol* 1985;6:327-41.
  28. Broekaert D, Coucke P, Leperque S, Ramaekers F, Van Muijen G, Boedts D, et al. Immunohistochemical analysis of the cytokeratin expression in middle ear cholesteatoma and related epithelial tissues. *Ann Otol Rhinol Laryngol* 1992;101:931-8.
  29. Huang CC, Chen CT, Huang TS, Shinoda H. Mediation of signal transduction in keratinocytes of human middle ear cholesteatoma by ras protein. *Eur Arch Otorhinolaryngol* 1996;253:385-9.
  30. Albino AP, Reed JA, Bogdany JK, Sassoon J, Desloge RB, Parisier SC. Expression of p53 protein in human middle ear cholesteatomas: pathogenetic implications. *Am J Otol* 1998;19:30-6.
  31. Akimoto R, Pawankar R, Yagi T, Baba S. Acquired and congenital cholesteatoma: determination of tumor necrosis factor-alpha, intercellular adhesion molecule-1, interleukin-1-alpha and lymphocyte functional antigen-1 in the inflammatory process. *ORL J Otorhinolaryngol Relat Spec* 2000;62:257-65.
  32. Kojima H, Miyazaki H, Shiwa M, Tanaka Y, Moriyama H. Molecular biological diagnosis of congenital and acquired cholesteatoma on the basis of differences in telomere length. *Laryngoscope* 2001;111:867-73.
  33. Kuczkowski J, Bakowska A, Pawelczyk T, Narozny W, Mikaszewski B. Cell cycle inhibitory protein p27 in human middle ear cholesteatoma. *ORL J Otorhinolaryngol Relat Spec* 2006;68:296-301.
  34. Park HR, Min SK, Min K, Jun SY, Seo J, Kim HJ. Increased expression of p63 and survivin in cholesteatomas. *Acta Otolaryngol* 2009;129:268-72.
  35. Haruyama T, Furukawa M, Kusunoki T, Onoda J, Ikeda K. Expression of IL-17 and its role in bone destruction in human middle ear cholesteatoma. *ORL J Otorhinolaryngol Relat Spec* 2010;72:325-31.
  36. Sikka K, Sharma SC, Thakar A, Dattagupta S. Evaluation of epithelial proliferation in paediatric and adult cholesteatomas using the Ki-67 proliferation marker. *J Laryngol Otol* 2012;126:460-3.
  37. Wang RG, Hawke M, Kwok P. The epidermoid formation (Michaels' structure) in the developing middle ear. *J Otolaryngol* 1987;16:327-30.
  38. Michaels L. Evolution of the epidermoid formation and its role in the development of the middle ear and tympanic membrane during the first trimester. *J Otolaryngol* 1988;17:22-8.
  39. Michaels L. Origin of congenital cholesteatoma from a normally occurring epidermoid rest in the developing middle ear. *Int J Pediatr Otorhinolaryngol* 1988;15:51-65.
  40. Michaels L, Soucek S. Stratified squamous epithelium in relation to the tympanic membrane: its development and kinetics. *Int J Pediatr Otorhinolaryngol* 1991;22:135-49.
  41. Kim JL, Jung HH. Proteomic analysis of cholesteatoma. *Acta Otolaryngol*

- 2004;124:783-8.
42. Mayans O, van der Ven PF, Wilm M, Mues A, Young P, Furst DO, et al. Structural basis for activation of the titin kinase domain during myofibrillogenesis. *Nature* 1998;395:863-9.
  43. Marx SO, Reiken S, Hisamatsu Y, Jayaraman T, Burkhoff D, Rosemblyt N, et al. PKA phosphorylation dissociates FKBP12.6 from the calcium release channel (ryanodine receptor): defective regulation in failing hearts. *Cell* 2000;101:365-76.
  44. Wright NT, Prosser BL, Varney KM, Zimmer DB, Schneider MF, Weber DJ. S100A1 and calmodulin compete for the same binding site on ryanodine receptor. *J Biol Chem* 2008;283:26676-83.
  45. David M. "Leucine scissors", *Glossary of Biochemistry and Molecular Biology* (Revised ed.). London: Portland Press; 1997.
  46. Koster J, Geerts D, Favre B, Borradori L, Sonnenberg A. Analysis of the interactions between BP180, BP230, plectin and the integrin alpha6beta4 important for hemidesmosome assembly. *J Cell Sci* 2003;116:387-99.
  47. Gundesli H, Talim B, Korkusuz P, Balci-Hayta B, Cirak S, Akarsu NA, et al. Mutation in exon 1f of PLEC, leading to disruption of plectin isoform 1f, causes autosomal-recessive limb-girdle muscular dystrophy. *Am J Hum Genet* 2010;87:834-41.
  48. Hromas R, Moore J, Johnston T, Socha C, Klemsz M. Drosophila forkhead homologues are expressed in a lineage-restricted manner in human hematopoietic cells. *Blood* 1993;81:2854-9.
  49. Peng SL. Forkhead transcription factors in chronic inflammation. *Int J Biochem Cell Biol* 2010;42:482-5.
  50. Friedland DR, Eernisse R, Erbe C, Gupta N, Cioffi JA. Cholesteatoma growth and proliferation: posttranscriptional regulation by microRNA-21. *Otol Neurotol* 2009;30:998-1005.
  51. Hromas R, Costa R. The hepatocyte nuclear factor-3/forkhead transcription regulatory family in development, inflammation, and neoplasia. *Crit Rev Oncol Hematol* 1995;20:129-40.
  52. Sutton J, Costa R, Klug M, Field L, Xu D, Largaespada DA, et al. Genesis, a winged helix transcriptional repressor with expression restricted to embryonic stem cells. *J Biol Chem* 1996;271:23126-33.
  53. Stetak A, Veress R, Ovadi J, Csermely P, Keri G, Ullrich A. Nuclear translocation of the tumor marker pyruvate kinase M2 induces programmed cell death. *Cancer Res* 2007;67:1602-8.
  54. Lee J, Kim HK, Han YM, Kim J. Pyruvate kinase isozyme type M2 (PKM2) interacts and cooperates with Oct-4 in regulating transcription. *Int J Biochem Cell Biol* 2008;40:1043-54.
  55. Luo W, Hu H, Chang R, Zhong J, Knabel M, O'Meally R, et al. Pyruvate kinase M2 is a PHD3-stimulated coactivator for hypoxia-inducible factor 1. *Cell* 2011;145:732-44.
  56. Miyagawa K, Tsuruga T, Kinomura A, Usui K, Katsura M, Tashiro S, et al. A role for RAD54B in homologous recombination in human cells. *Embo j* 2002;21:175-80.
  57. Tanaka K, Kagawa W, Kinebuchi T, Kurumizaka H, Miyagawa K. Human Rad54B is a double-stranded DNA-dependent ATPase and has biochemical

- properties different from its structural homolog in yeast, Tid1/Rdh54. *Nucleic Acids Res* 2002;30:1346-53.
58. Martinsson H, Yhr M, Enerback C. Expression patterns of S100A7 (psoriasin) and S100A9 (calgranulin-B) in keratinocyte differentiation. *Exp Dermatol* 2005;14:161-8.
  59. Celis JE, Rasmussen HH, Vorum H, Madsen P, Honore B, Wolf H, et al. Bladder squamous cell carcinomas express psoriasin and externalize it to the urine. *J Urol* 1996;155:2105-12.
  60. Munday NA, Vaillancourt JP, Ali A, Casano FJ, Miller DK, Molineaux SM, et al. Molecular cloning and pro-apoptotic activity of ICErelII and ICErelIII, members of the ICE/CED-3 family of cysteine proteases. *J Biol Chem* 1995;270:15870-6.

ABSTRACT (IN KOREAN)

프로테오믹스 분석을 통해 선천성 진주종, 후천성 진주종 및  
외이도 피부에 발현되는 단백질의 비교로 선천성 진주종의  
병인에 관한 연구

<지도교수 최 재 영>

연세대학교 대학원 의학과

신 승 호

선천성 진주종은 파괴적인 성장과 골용해를 보이는 상피성 병변이다. 발생률은 중이 진주종의 1-5%이지만, 발견률이 증가 추세이다. 선천성 진주종은 적절히 치료되지 않는 경우, 특히 청력을 손상시킬 수 있다. 후천성 진주종의 분자화학적 연구가 어느 정도 진행되어 있으나, 선천성 진주종에 대한 연구는 매우 적다. 그래서 선천성 진주종에 대한 분자화학적 연구가 현재 필요하다. 유전학적 연구의 제한점을 고려했을 때, 프로테오믹스를 이용해 선천성 진주종에 발현되는 단백질의 교차연구가 선천성 진주종의 병인을 이해와 치료의 발전에 도움을 줄 수 있을 것이다.

수술 중 얻은 선천성 진주종 4례와 외이도 피부 4례, 2례의 후천성 진주종이 사용되었다. 2차원 전기영동을 통해 분자량에 따라 단백질을 분리하였다. 분리된 단백질 중 선천성 진주종에서만 많이 발현되는 10개의 단백질을 MALDI-TOF MS와 면역염색을 통해 분석하였다.

**결과:** 2D 전기 영동에서 선천성 진주종 4례는 매우 비슷한 단백질 분포를 보였다. 후천성 진주종과 선천성 진주종의 발현된 단백질을 비교했을 때, 어떤 단백질은 공통으로 발현이 되었고 다른 단백질은

그렇지 않았다. 선천성 진주종과 외이도피부에 발현된 단백질 역시 공통적으로 발현된 단백질과 그렇지 않은 단백질로 구분이 되었다. 선천성 진주종, 후천성 진주종 그리고 외이도 피부에서 발견된 단백질의 개수는 각각 556, 460 그리고 624 개이다. 선천성 진주종과 후천성 진주종에서 동시에 발견된 단백질의 개수는 326개이며 이 중 56개의 단백질은 외이도 피부에서 발현되지 않았다. 피부와 선천성 진주종에서 동시에 발견된 단백질의 개수는 373개이다. 종합하면 127개의 단백질이 선천성 진주종에서만 발견이 되었다. 후천성 진주종에서 발현된 것보다 더 많이 발현된 선천성 진주종 상위 10개의 단백질은 titin (gi|407139), PRO2619 (gi|11493459), forkhead transcription activator homolog (gi|477361), ryanodine receptor 2 (cardiac), isoform CRA\_c (gi|119590477), plectin 1, intermediate filament binding protein (gi|119602578), keratin 10 (epidermolytic hyperkeratosis; keratosis palmaris et plantaris, gi|119581085), keratin 10 (gi|186629), keratin 10 (gi|119581085), titin (gi|407139), leucine zipper protein 5 그리고 isoform CRA\_b (gi|119624991)이었다. 또, 피부에서는 발현되지 않고 후천성 진주종보다 과발현된 선천성 진주종의 단백질 9개를 분석한 결과 Ig heavy chain variable region (gi|951281), chain A structure of human muscle pyruvate kinase (Pkm2, gi|67464392), ribosomal protein L35a isoform CRA\_c (gi|119612656), DNA repair and recombination protein RAD54B isoform 3 (gi|327532753), protein S100-A7 (gi|115298657), caspase-5/f (gi|81170715), chain B crystal structure of human caspase-2 in complex with Acetyl-Leu-Asp-Glu-Ser-Asp-Cho (gi|34810359), cyclic nucleotide gated channel beta 3 (gi|223462173) 등이 확인되었다.

면역염색상 forkhead transcription activator homolog (FKH 5-3), keratin-10, titin 등이 선천성 진주종 시료에서 확인이 되었다.

이 연구에서 후천성 진주종과 외이도 피부와는 달리 선천성 진주종에서만 발견되는 단백질들을 발견하였다. 이 단백질들 중 일부는 선천성 진주종의 병태생리에 중요한 역할을 할 것으로 보인다. 그러나 이들에 대한 기능적 연구를 더 이루어져야 한다.

---

핵심되는 말: 선천성 진주종, 후천성 진주종, 외이도 피부,  
프로테오믹스, 면역염색